OPEN ACCESS **MOLECULES** ISSN 1420-3049 www.mdpi.com/journal/molecules

Article

[15]aneN₄S: Synthesis, Thermodynamic Studies and Potential Applications in Chelation Therapy

Nuno Torres¹, Sandrina Gonçalves¹, Ana S. Fernandes², J. Franco Machado¹, Maria J. Villa de Brito^{3,4}, Nuno G. Oliveira¹, Matilde Castro¹, Judite Costa^{1,†} and Maria F. Cabral^{1,†,*}

- ¹ Instituto de Investigação do Medicamento (iMed.ULisboa), Faculdade de Farmácia, Universidade de Lisboa, Av. Prof. Gama Pinto, Lisboa 1649-003, Portugal; E-Mails: nunotorr@gmail.com (N.T.); sandrinagoncalves@campus.ul.pt (S.G.); joaomachado@campus.ul.pt (J.F.M.); ngoliveira@ff.ul.pt (N.G.O.); mcastro@ff.ul.pt (M.C.); jcosta@ff.ul.pt (J.C.)
- ² CBIOS, Universidade Lusófona Research Center in Biosciences & Health Technologies, Campo Grande 376, Lisboa 1749-024, Portugal; E-Mail: ana.fernandes@ulusofona.pt
- ³ CQE, Instituto Superior Técnico, Universidade de Lisboa, Av. Rovisco Pais, Lisboa 1049-001, Portugal; E-Mail: mjbrito@fc.ul.pt
- ⁴ DQB, Faculdade de Ciências, Universidade de Lisboa, Campo Grande, Lisboa 1749-001, Portugal
- [†] These authors contributed equally to the senior authorship.
- * Author to whom correspondence should be addressed; E-Mail: fcabral@ff.ul.pt; Tel.: +351-217-946-400; Fax: +351-217-946-470.

Received: 2 December 2013; in revised form: 23 December 2013 / Accepted: 24 December 2013 / Published: 3 January 2014

Abstract: The purpose of this work was to synthesize and characterize the thiatetraaza macrocycle 1-thia-4,7,10,13-tetraazacyclopentadecane ([15]aneN₄S). Its acid-base behaviour was studied by potentiometry at 25 °C and ionic strength 0.10 M in KNO₃. The protonation sequence of this ligand was investigated by ¹H-NMR titration that also allowed the determination of protonation constants in D₂O. Binding studies of [15]aneN₄S with Mn^{2+} , Fe²⁺, Co²⁺, Ni²⁺, Cu²⁺, Zn²⁺, Cd²⁺, Hg²⁺ and Pb²⁺ metal ions were further performed under the same experimental conditions. The results demonstrated that this compound has a higher selectivity and thermodynamic stability for Hg²⁺ and Cu²⁺, followed by Ni²⁺. The UV-visible-near IR spectroscopies and magnetic moment data for the Co(II) and Ni(II) complexes indicated a tetragonal distorted coordination geometry for both metal centres.

The value of magnetic moment and the X-band EPR spectra of the Cu(II) complex are consistent with a distorted square pyramidal geometry.

Keywords: macrocyclic compounds; thiatetraaza; stability constants; spectroscopic studies; chelation therapy; mercury(II) chelator; copper(II) chelator

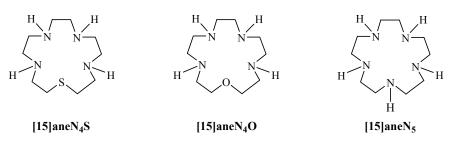
1. Introduction

Exposure to toxic metals is associated with the potential development of numerous health effects, including different types of cancer [1,2]. Humans are exposed to metals and their compounds through environmental and occupational scenarios and also by food consumption, being the adverse effects dependent on dose, period of exposure and metal bioavailability [3]. In fact, metals can disturb the normal function of several organ systems and generate different toxicological effects through their excess, lack or imbalance [4]. The mainstay treatment against metal toxicity is chelation therapy [5,6], where appropriate chelators are used to remove metals from the organism [7], and thereby reduce toxicity [8,9]. However, despite the available chelators, the search for new effective chelating compounds is still needed, since the ones currently used in clinic present a number of toxic side effects, low metal specificity and controversial efficacy [5,9,10].

Previously, we have explored the possible use of macrocyclic compounds for medical applications, namely in chelation therapy [7,11]. These compounds may exhibit important properties such as less toxicity, high kinetic and thermodynamic stabilities [12], rendering them very promising agents in this context. Macrocycles are also advantageous in terms of selectivity, since they have more rigid structures and can thus inflict specific coordination geometry to the metal ion, while open chain chelators can adapt more easily to the geometric requirements of the metal centre [7,13].

A large amount of data has been published on macrocyclic ligands containing only nitrogen, only sulphur or both as donor atoms, namely tetraaza- [13], thiadiaza- [14], thiatriaza- [15], dithiadiaza- [16–20], dithiatriaza- [20] or pentathia- macrocycles [15]. However, there is scarce information on thiatetraaza compounds. In fact, only one thiatetraaza macrocycle, 1-thia-4,7,11,14-tetraazacyclohexadecane, was studied [21]. In the present work, we investigate a 15-membered thiatetraaza macrocyclic compound, 1-thia-4,7,10,13-tetraazacyclopentadecane ([15]aneN₄S, Figure 1). In this context, we address the synthesis and characterization of [15]aneN₄S and assess its potential as a chelating agent. To accomplish this aim, the acid-base behaviour of this macrocycle was studied and its ability to specifically coordinate with several divalent ions was evaluated.

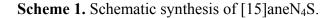
Figure 1. [15]aneN₄S, [15]aneN₄O and [15]aneN₅ macrocycles.

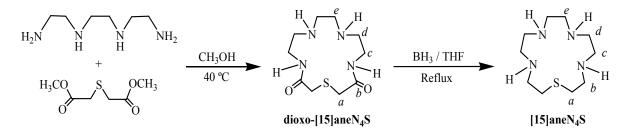


2. Results and Discussion

2.1. Synthesis and Characterization

The macrocycle 1-thia-4,7,10,13-tetraazacyclopentadecane ([15]aneN₄S) was prepared according to the reactions depicted in Scheme 1. The first step involved the synthesis of the precursor diamide, 1-thia-4,7,10,13-tetraazacyclopentadecane-3,14-dione (dioxo-[15]aneN₄S) by reaction of the dimethyl ester of thiodiglycolic acid, prepared according to a reported procedure [22], with triethylenetetramine in dry methanol at 40 °C, under N₂ for nine days. The general procedure was similar to those reported in the literature by Tabushi *et al.* [23] and by Steenland *et al.* [24], who obtained this macrocycle with 15% to 17% yield. However, some modifications were introduced in the present work, such as controlled reaction temperature, dried solvent in a larger volume and nitrogen atmosphere, which led to the highly improved yield of 74% on dioxo-[15]aneN₄S synthesis. The reduction of this cyclic diamide with borane, in refluxing dry THF under nitrogen for eight hours, afforded the [15]aneN₄S. After purification by chromatography, the trihydrocloride salt was obtained by addition of 37% HCl until pH \approx 2. A yield of 68% was obtained, which is within the range reported for similar compounds (60%–80%) [23].





The structure of the compound was confirmed by ¹H and ¹³C-NMR spectroscopy (Table S1 and Figures S1–S2 in Supplementary Materials). NMR data for [15]aneN₄S are consistent with a C_{2y} symmetric structure in solution, according to the number of signals observed in the ¹H and ¹³C-NMR spectra. Five resolved proton and carbon resonances were observed and a combination of the two-dimensional spectra HMBC, HMQC and COSY (Figures S3-S6 in Supplementary Materials), were used for the assignments. The singlet observed in the ¹H-NMR spectrum at δ 3.34 was assigned to H_e. C_d at 43.65 ppm was identified through ${}^{3}J$ correlation to H_e, which allowed the assignment of the coupled triplets H_d and H_c at 3.44 and 3.57 ppm, respectively. ³J C-H coupling of the more shielded CH_2 group to its symmetric counterpart, bridged by the sulphur atom, allowed the assignment of the resonances at δ 29.55 and 3.17 to C_a and H_a, respectively. The HMBC spectrum also exhibits three-bond CH correlation of H_b, at δ 3.50, to C_a and two-bond coupling to C_d. The two pairs of triplets in the ¹H-NMR spectrum display a nearly first-order A₂X₂ coupling pattern with some distortion. The resulting "roof effect" with a mirror image relationship is often observed for CH₂-CH₂ groups in an unsymmetrical environment with some strain. Leaning is more pronounced for the H_c/H_d pair which is closer in chemical shift ($\Delta\delta/\Delta J < 10$), leading to slightly different coupling constants. For the H_a/H_b spin system, second order effects are negligible due to the higher chemical shift difference ($\Delta\delta/\Delta J > 20$).

2.2. Acid-Base Behaviour

The acid-base behaviour of [15]aneN₄S was studied by potentiometry in water at 25 °C and ionic strength 0.10 M in KNO₃. This compound was also studied by ¹H-NMR spectroscopy. The determined protonation constants are collected in Table 1 together with the values of the related [15]aneN₄O and [15]aneN₅ compounds (Figure 1) for comparison. The ligand has four basic centres. However only three constants could be accurately determined by potentiometry and the fourth one was obtained by ¹H-NMR. The compound exhibits high and fairly high values respectively for the first two protonation constants corresponding to the protonation of nitrogen atoms in opposite positions, minimizing the electrostatic repulsion between positive charges of the ammonium groups formed. The third and fourth constants are much lower due to the stronger electrostatic repulsions as they correspond to protonation of nitrogen atoms at short distances from already protonated ones, and to the limited motion allowed in the ring backbone.

The overall basicity and all the stepwise protonation constants of [15]aneN₄S (Table 1) are slightly lower than those of [15]aneN₄O but even lower than those of [15]aneN₅, as expected. Indeed sulphur and oxygen atoms have different electronic characteristics with respect to amino groups. Evidently, ethereal S and O cannot bind acidic protons, if not under particular conditions; they have different inductive effects on the adjacent aliphatic chains with respect to nitrogen and finally, they have a much lower tendency to form hydrogen bonds and are less solvated in aqueous solution than amino groups [25]. Considering these features, the introduction of S or O in the macrocyclic backbone may deeply influence the basicity of these molecules. The lower stabilization via intramolecular hydrogen bonds formation brought about by S and O in the mono and/or polyprotonated species gives rise to a consequent basicity decrease with respect to the corresponding unsubstituted polyazacycloalkanes [25].

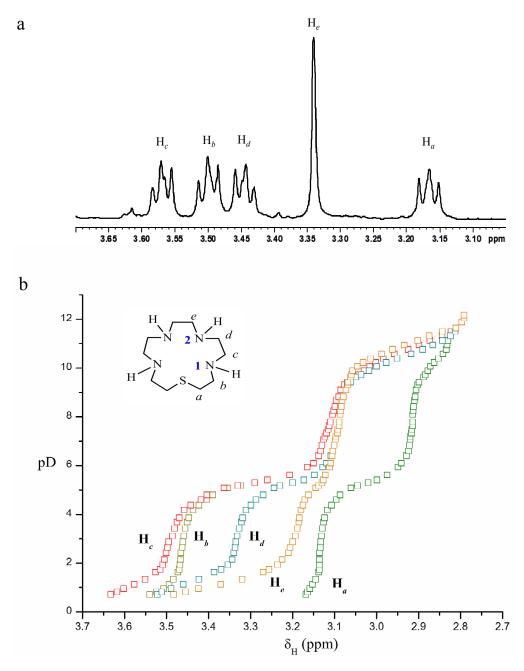
Reaction equilibrium	[15]aneN ₄ S ^{a,b}	[15]aneN ₄ O ^c	[15]aneN ₅ ^d
$\Gamma + H_{+}^{+} \rightleftharpoons H\Gamma_{+}^{+}$	9.51(1)	9.66	10.01
$\mathrm{HL}^{+} + \mathrm{H}^{+} \rightleftharpoons \mathrm{H}_{2}\mathrm{L}^{2+}$	8.56(2)	8.77	9.28
$H_2L^{2+} + H^+ \rightleftharpoons H_3L^{3+}$	4.47(4)	5.30	5.87
$H_3L^{3+} + H^+ \rightleftharpoons H_4L^{4+}$	0.8(2) ^e	1.2	1.84
$L + 4 H^+ \rightleftharpoons H_4 L^{4+}$	23.34	24.93	27.00

Table 1. Stepwise protonation constants (log K_i^H) of [15]aneN₄S and similar compounds.

^a Values in parentheses are standard deviations on the last significant figure. ^b Present work T = 25.0 °C; I = 0.10 M in KNO₃. ^c T = 25.0 °C; I = 0.10 M in KNO₃; ref. [26]. ^d T = 25.0 °C; I = 0.10 M in KCl; ref. [27]. ^e Determined in this work by ¹H-NMR spectroscopy, using the calculated value of pK_{D4} and the equation $pK_D = 0.11 + 1.10 \times pK_H$; ref. [28].

¹H-NMR spectroscopic titration of [15]aneN₄S was carried out in order to understand its protonation sequence and to determine the lower protonation constant. The ¹H-NMR spectrum of the compound at pD 1.72 (Figure S1) and the titration curves are shown in Figure 2a,b, respectively. In the 0.72 to 4.80 pD region, five resonances were observed in the ¹H-NMR spectra. The H_c and H_b resonances overlap for pD values above 5.09 until 12.17. The same behaviour was observed for the H_e and H_d resonances between 6.40 and 9.42. The triplets at 3.57, 3.50, 3.44 and 3.17 ppm were assigned to protons H_c, H_b, H_d and H_a, respectively, and the singlet at 3.34 ppm corresponds to H_e. (Figure 2a).

Figure 2. (a) ¹H-NMR spectrum of [15]aneN₄S in D₂O, pD 1.72; (b) ¹H-NMR titration curves for [15]aneN₄S, chemical shift $\delta_{\rm H}$ (ppm) in function of pD.



The ¹H-NMR titration curves (Figure 2b) show the effect of successive protonation of the basic centres of the molecule on the chemical shifts of the protons. The first two equivalents of acid added to the basic form of the ligand (pD 11.65–9.31) affected the four N–atoms of the compound, as all the resonances shift downfield in this pD region. The first equivalent protonates mainly N²–centres, since the H_e resonance undergoes a larger downfield shift, followed by H_d, H_c, H_b and H_a, meaning a small degree of protonation of N¹–atoms. The second equivalent of acid protonates mainly N¹–centres, as H_a, H_b and H_c resonances move downfield, although simultaneous protonation of N²–centres is also evident, since H_d and H_e resonances show downfield shifts as well.

The third equivalent of acid (pD 5.94–3.69) continues protonating the N¹–centres, since H_a , H_b and H_c signals show a significant shift downfield. However, a smaller downfield shift of H_d and H_e

resonances is also observed, revealing some degree of protonation on N²–centres still occurring. Addition of one more equivalent of acid (pD < 2.15) causes protonation on N² centres at a larger extent, according to the larger downfield shift observed for the H_e and H_d resonances. The last protonation occurs in a centre at a very short distance from others already protonated, and the strong repulsions then aroused in the molecule, where the motion is limited by the skeleton of the ring, renders the protonation difficult.

The ¹H-NMR titration also allowed the determination of the protonation constants in D₂O for [15]aneN₄S: $pK_{D1} = 10.90(7)$, $pK_{D2} = 9.4(1)$, $pK_{D3} = 5.3(1)$ and $pK_{D4} = 1.0(1)$. These values are in agreement with the equation for the correlation between the protonation constants determined in H₂O and in D₂O for similar compounds: $pK_D = 0.11 + 1.10 \times pK_H$ [28].

2.3. Thermodynamic Stability of Metal Complexes

The stability constants of [15]aneN₄S with Mn²⁺, Fe²⁺, Co²⁺, Ni²⁺, Cu²⁺, Zn²⁺, Cd²⁺, Hg²⁺ and Pb²⁺, determined by potentiometric titrations at 25 °C and ionic strength 0.1 M in KNO₃, are collected in Table 2 together with the corresponding constants of complexes of the related macrocycles [15]aneN₄O [26,29] and [15]aneN₅ [30–33] taken from the literature for comparison. Only mononuclear ML, M(HL) and ML(OH) complexes were found. In the case of Hg²⁺ and Mn²⁺, the protonated species were not formed under our experimental conditions. For Co²⁺ and Ni²⁺, the determination of the stability constants for hydroxocomplexes was precluded since precipitation occurred (Table 2). In all cases the proposed model was accepted by the HYPERQUAD program [34] using all data points from all titration curves, with good statistical parameters.

Reaction equilibrium	[15]aneN ₄ S ^{a,b}	[15]aneN ₄ O ^c	[15]aneN ₅ ^d		
$Mn^{2+} + L \rightleftharpoons MnL^{2+}$	6.65(2)	8.53 °	10.85 ^e		
$MnL^{2+} + H^{+} \rightleftharpoons MnHL^{3+}$	-	-	5.04 ^e		
$MnL(OH)^{+} + H^{+} \rightleftharpoons MnL^{2+}$	9.68(4)	-	11.22 ^e		
$Fe^{2+} + L \rightleftharpoons FeL^{2+}$	10.08(1)	10.34 ^c	-		
$\operatorname{FeL}^{2+} + \operatorname{H}^{+} \rightleftharpoons \operatorname{FeHL}^{3+}$	4.83(6)	-	-		
$\operatorname{FeL(OH)}^{+} + \operatorname{H}^{+} \rightleftharpoons \operatorname{FeL}^{2+}$	8.25(7)	pp.	-		
$\mathrm{Co}^{2^+} + \mathrm{L} \rightleftharpoons \mathrm{CoL}^{2^+}$	13.62(6)	12.72 ^c	16.76 ^f		
$CoL^{2+} + H^{+} \rightleftharpoons CoHL^{3+}$	5.20(7)	-	-		
$Ni^{2+} + L \rightleftharpoons NiL^{2+}$	17.95(5)	14.76 ^c	18.1 ^g		
$NiL^{2+} + H^+ \rightleftharpoons NiHL^{3+}$	4.00(7)	-	-		
$NiL(OH)^{+} + H^{+} \rightleftharpoons NiL^{2+}$	-	8.38 ^c	-		
$Cu^{2+} + L \rightleftharpoons CuL^{2+}$	22.31(2)	20.34 ^c	28.0 ^h		
$CuL^{2+} + H^{+} \rightleftharpoons CuHL^{3+}$	2.49(5)	-	-		
$CuL(OH)^{+} + H^{+} \rightleftharpoons CuL^{2+}$	9.8(1)	10.4 ^c	-		
$Zn^{2+} + L \rightleftharpoons ZnL^{2+}$	13.472(8)	13.21 ^c	19.1 ⁱ		
$\operatorname{ZnL}^{2+} + \operatorname{H}^{+} \rightleftharpoons \operatorname{ZnHL}^{3+}$	4.06(3)	-	3.1 ⁱ		
$\operatorname{ZnL}(\operatorname{OH})^+ + \operatorname{H}^+ \rightleftharpoons \operatorname{ZnL}^{2+}$	7.16(4)	-	-		

Table 2. Stepwise stability constants (log units) of the complexes of $[15]aneN_4S$, $[15]aneN_4O$ and $[15]aneN_5$ with different metal ions.

Reaction equilibrium	[15]aneN ₄ S ^{a,b}	[15]aneN ₄ O ^c	[15]aneN ₅ ^d
$Cd^{2+} + L \rightleftharpoons CdL^{2+}$	13.61(2)	13.41 ^d	19.2 ⁱ
$CdL^{2+} + H^{+} \rightleftharpoons CdHL^{3+}$	3.97(4)	-	3.4 ⁱ
$CdL(OH)^{+} + H^{+} \rightleftharpoons CdL^{2+}$	9.25(7)	-	-
$Hg^{2+} + L \rightleftharpoons HgL^{2+}$	23.74(5)	-	28.5 ^j
$HgL(OH)^{+} + H^{+} \rightleftharpoons HgL^{2+}$	10.3(1)	-	-
$Pb^{2+} + L \rightleftharpoons PbL^{2+}$	12.44(2)	12.28 ^d	17.3 ⁱ
$PbL^{2+} + H^+ \rightleftharpoons PbHL^{3+}$	4.44(4)	-	3.8 ⁱ
$PbL(OH)^{+} + H^{+} \rightleftharpoons PbL^{2+}$	7.76(7)	-	-

Table 2. Cont.

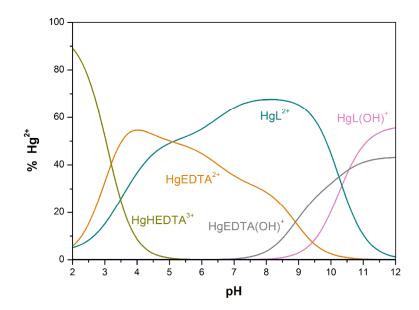
^a Values in parentheses are standard deviations on the last significant figure. ^b Present work T = 25.0 °C; I = 0.10 M in KNO₃. ^c T = 25.0 °C; I = 0.10 M in KNO₃; ref. [26]. ^d T = 25.0 °C; I = 0.10 M in NaNO₃; ref. [29]. ^e T = 25.0 °C; I = 0.10 M in NaClO₄; ref. [30]. ^f T = 35.0 °C; I = 0.20 M in NaClO₄; ref. [31]. ^g T = 35.0 °C; ref. [32]. ^h T = 25.0 °C; I = 0.2 M; polarographic method; ref. [35]. ⁱ T = 25.0 °C; I = 0.2 M; ref. [33]. ^j T = 25.0 °C; I = 0.2 M; polarographic method; ref. [33].

Potentiometric studies with [15]aneN₄S and $Ca(NO_3)_2$ showed that both titration curves (protonation and complexation at a molar ratio 1:1) overlapped, suggesting that Ca^{2+} does not bind to the ligand. This hypothesis was supported by NMR data, as no changes were observed in the ¹H-NMR spectrum of the ligand in presence of Ca^{2+} .

Direct determinations of the stability constants of Cu[15]aneN₄S²⁺ and Hg[15]aneN₄S²⁺ were not possible as ML²⁺ was almost completely or completely formed in the beginning of the titration (pH ≈ 2.2) (Figures S9 and S11 in Supplementary Materials, respectively). Consequently, reliable values for the constants were obtained through a competition with a reference ligand, for which the protonation and stability constants are accurately known [36]. Among the various ligands tried, H₄EDTA was chosen as the best reference ligand. Figure 3 shows the species distribution diagram of the ligand-ligand competition reaction between [15]aneN₄S, Hg²⁺ and ethylenediaminetetraacetic acid (EDTA), obtained with the HySS program [37]. In the Supplementary Materials the species distribution curves for Cu(II) competition titration are shown (Figure S10).

[15]aneN₄S is very selective, exhibiting a very high stability constant for Cu²⁺ (log $K_{ML} = 22.31$), and a fairly high value for Ni²⁺ (log $K_{ML} = 17.95$). On the other hand, the stability constants for the complexes of the remaining first-row transition metal ions decrease sharply. The Cd²⁺ and Pb²⁺ complexes have low stabilities. Hg²⁺ has the highest stability constant (log $K_{ML} = 23.74$) of all the metal ions studied.

In spite of the slightly lower overall basicity of [15]aneN₄S, this ligand forms ML^{2+} complexes more stable than those of the oxatetraaza macrocycle [15]aneN₄O, except in the case of the Mn²⁺and Fe²⁺complexes (variations of 1.88 and 0.26 log units, respectively). [15]aneN₄S is particularly advantageous over [15]aneN₄O for Ni²⁺ and Cu²⁺complexes, being the stability constants much higher (an increase of 3.19 and 1.97 log units, respectively, was found). Comparing with the pentaaza macrocycle [15]aneN₅, the stability constants (log values) of the ML²⁺ metal complexes of [15]aneN₄S are smaller except in the case of the Ni²⁺ complexes which have almost the same value (Table 2). **Figure 3.** Species distribution curves calculated for an aqueous solution containing [15]aneN₄S (L), Hg²⁺ and EDTA at 0.75:1:1 molar ratio. Percentages are given relative to Hg²⁺ at an initial value of 1.73×10^{-3} M.



However, stability constants do not provide directly comparable basis for the measuring of total ion sequestering abilities of the ligands at physiological conditions (pH 7.4) and therefore they were used to calculate the pM values, defined as $-\log [M^{2+}]$ (Table 3). The advantage of comparing pM values rather than stability constants is that the pM values reflect the influence of ligand basicity and metal chelate protonation.

Table 3. pM	values	calculated	for	metal	complexes	of [15]aneN ₄ S,	[15]aneN ₄ O	and
[15]aneN5 at p	H 7.4 ^a .							

Metal ion	[15]aneN ₄ S	[15]aneN₄O	[15]aneN5		
Mn ²⁺	5.02	5.31	6.38		
Fe ²⁺	6.85	5.74	-		
Co ²⁺	10.32	9.07	12.25		
Ni ²⁺	14.65	11.15	13.59		
Cu^{2+}	19.01	16.69	23.49		
Zn^{2+}	10.61	9.56	14.59		
Cd^{2^+}	10.32	9.76	14.69		
Hg^{2+} Pb^{2+}	20.44	-	23.99		
Pb^{2+}	9.3	8.63	12.79		

^a Values calculated for 100% molar excess of the ligand over the metal ion with $C_M = 1.0 \times 10^{-5}$ M, based on the protonation constants and stability constants of Tables 1 and 2, using the HySS program; ref. [37].

If the pM values of [15]aneN₄S are compared with those of [15]aneN₄O (Table 3) we conclude that, with the exception of Mn^{2+} , all the values are higher, especially for nickel(II) and copper(II) complexes (differences, in log units, are 3.5 and 2.32, respectively). On the other hand, the comparison of pM values of the metal complexes of [15]aneN₄S with [15]aneN₅ (Table 3) revealed that the former complexes present lower values, except in the case of the Ni²⁺ complex, which has a higher value

2.4. Spectroscopic Studies

UV-visible-near IR spectroscopic studies of the Co(II), Ni(II) and Cu(II) complexes of [15]aneN₄S in water solution were performed and the magnetic moments determined by the Evans method [38]. The results are collected in Table 4.

The electronic spectrum of the pink Co[15]aneN₄S²⁺ exhibits two principal bands, at 1075 and 504 nm, and four shoulders (Table 4), consistent with a high-spin octahedral array tetragonally distorted around the Co(II) ion [39] with one water molecule or a metal counter-ion nitrate occupying a coordination site. The octahedral field splitting parameter 10Dq [39] of 11450 cm⁻¹ is in the expected range for relatively weak ligands. The band at 504 nm is more intense than expected for forbidden transitions in O_h complexes, which can be explained by the loss of symmetry caused by distortion. The magnetic moment of 4.9 MB is within the range for high-spin six coordinate Co(II) complexes [38]. Although five coordinate Co(II) species would also have a similar value, the absence of a weak absorption in the visible region between 830 and 670 nm, characteristic of five coordinate Co(II) complexes [39–41], supports the proposed six coordination for this metal ion.

Complex; (colour)	рН	UV-visible-near IR ^a $\lambda_{max}/nm (\epsilon, M^{-1} cm^{-1})$	μ (MB)			
Co[15]aneN ₄ S ²⁺ (pink)	6.99	1075 (4.2), 970 (sh., 4.9), 504 (67.6), 491 (sh., 99.0), 325 (sh., 2.61×10^3), 270 (sh., 2.61×10^3).	4.9			
Ni[15]aneN ₄ S ²⁺ (yellow)	6.98	1040 (2.12), 945 (23.0), 847 (sh., 27.2), 813 (sh., 26.0), 528 (19.3), 310 (sh., 1.49 × 10 ³), 264 (1.91 × 10 ⁴).	3.1			
Cu[15]aneN ₄ S ²⁺ (purple)	7.08	977 (23.8), 748 (sh., 16.3), 562 (45.6), 273 (1.17 × 10 ³).	1.8			
	^a sh. = shoulder.					

Table 4. Spectroscopic UV-visible-near IR data and magnetic moments (μ) for the Co(II), Ni(II) and Cu(II) complexes of [15]aneN₄S.

The electronic spectrum of the yellow Ni[15]aneN₄S²⁺ shows three absorption bands of low intensity in the visible-near IR regions and a charge transfer band at 264 nm (Table 4).

Taking into account the work of Busch *et al.* [42], we assigned the two bands in the visible-near IR regions to transitions ${}^{3}B_{1g} \rightarrow {}^{3}B_{2g}$, (directly related to $10Dq^{xy}$) and ${}^{3}B_{1g} \rightarrow {}^{3}E_{g}^{a}$ (equal to the difference between $10Dq^{xy}$ and $35/4D_{t}$). The octahedral field splitting parameter 10Dq and the values of the equatorial (Dq^{xy}) and axial (Dq^{z}) ligand field were calculated according to those assignments: $10Dq = 18975 \text{ cm}^{-1}$, $Dq^{xy} = 1898 \text{ cm}^{-1}$ and $Dq^{z} = 219 \text{ cm}^{-1}$. These values, together with the ratio v_1/v_2 of 1.79 (v_1 and v_2 being the near IR and the visible absorption bands, respectively) and the magnetic moment of 3.1 MB, are characteristic of six coordinate nickel(II) environments, indicating a tetragonal (D_{4h}) distorted octahedral geometry for this complex [43].

The purple Cu[15]aneN₄S²⁺ complex exhibits a broad band in the visible region with the maximum centred at 565 nm assigned to the copper *d*-*d* transition, an intense band in the UV region and a small broad band in the near IR region (Table 4).

The X-band EPR spectra of Cu[15]aneN₄S²⁺ at the 1:1 ratio in water solution are shown in Figure 4 at three pH values. The spectra are very similar and suggest the presence of only one species. Spectroscopic visible data (λ_{max}), the hyperfine coupling constants A_i and g values, determined by the simulation of the spectra [44] (Figure 4) are compiled in Table 5 together with those of the related complex Cu[15]aneN₄O²⁺, from the literature [45].

Figure 4. EPR X-band spectra of Cu(II) complex of [15]aneN₄S in 1:1 ratio at pH 4.10 (**a**), 7.40 (**b**) and 9.00 (**c**) in 1.0 M of NaClO₄. The spectra were recorded at 104 K, microwave power of 2.0 mW and modulation amplitude of 1.0 mT. The frequency (v) was of 9.67 GHz. The simulated spectra (red lines) are below of the experimental ones (black lines).

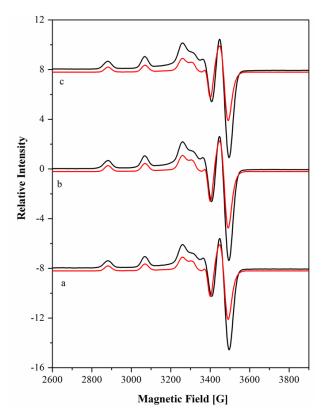


Table 5. Spectroscopic X-band EPR data for the Cu(II) complexes of $[15]aneN_4S^a$ and the related ligand $[15]aneN_4O$.

Complex	рН	Visible band λ_{max}/nm (ϵ_{molar} , M^{-1} cm ⁻¹)	EPR parameters ($A_i \times 10^4 \text{ cm}^{-1}$)						
			g_x	g_y	g_z	A_x	A_y	A_z	ref.
	9.00		2.043	2.046	2.186	30.6	28.7	192.5	-
$Cu[15]aneN_4S^{2+}$	7.40	565 (46)	2.042	2.045	2.182	30.3	28.0	191.1	-
	4.10		2.041	2.042	2.185	30.4	28.0	191.3	-
Cu[15]aneN ₄ O ²⁺	7.41	580 (141)	2.042	2.046	2.192	30.0	27.9	199.4	[45]

^a This work.

The parameters obtained for $Cu[15]aneN_4S^{2+}$ are characteristic of mononuclear copper(II) complexes in rhombic geometry with elongation of the axial bonds and a $d_{x^2-y^2}$ ground state, consistent with distorted octahedral (with the sixth coordination site occupied by one water molecule or a metal counter-ion nitrate) or square pyramidal environment. Trigonal bipyramidal or tetragonal geometries involving compression of axial bonds should be excluded [46–48].

The hyperfine constants A_i and g values are related to the electronic transitions by the factors derived from the ligand field theory [49–51]: the g_z values increase and the A_z values decrease when the planar ligand field becomes weaker or the axial ligand field becomes stronger, and this occurs with the simultaneous red-shift of the *d*-*d* absorption bands in the electronic spectra. This sequence parallels the degree of distortion from square planar to square pyramidal (C_{4v}) and then to octahedral (O_h) or tetragonal (D_{4h}) geometries [47].

The EPR parameters and the electronic spectra data for the complex $Cu[15]aneN_4S^{2+}$ are similar to those obtained for $Cu[15]aneN_4O^{2+}$ (Table 5), for which a square pyramidal geometry around the copper ion was proposed, with the four nitrogen atoms in the equatorial plane and the oxygen atom occupying the apical position [45]. The $Cu[15]aneN_4S^{2+}$ complex presents slightly lower g_z values and a small blue-shift of the absorption band, consistent with a slightly stronger equatorial ligand field. Although the coordination geometry of the complex cannot be unequivocally established without an X-ray structure, the similar results for both compounds suggest for $Cu[15]aneN_4S^{2+}$ a distorted square pyramidal environment around the Cu(II) centre, with the sulphur atom in the apical position and the four nitrogen atoms in the equatorial plane.

3. Experimental

3.1. General

FT-IR spectra were recorded in a Nicolet 6700 FT-IR spectrophotometer (Thermo Electron Corporation, Runcord, UK) using KBr pellets. Electrospray ionization-mass spectrometry (ESI-MS) was carried out with a Micromass Quattro Micro triple quadrupole instrument (Waters, Milford, MA, USA) and MassLynx software (version 4.1) was used for data analysis. The ionization of the compound was performed by an electrospray source in positive mode (ESI+). UV-visible spectra were recorded with a UNICAM UV-4 (Thermo Scientific, Waltham, MA, USA) and UV-visible-near IR spectra were collected with a Shimadzu UV-1603 (Tokyo, Japan). EPR spectroscopic measurements were recorded with a Bruker ESP EMX 300 spectrometer (Bruker BioSpin GmbH, Rheinstetten, Germany) equipped with continuous-flow cryostats for liquid nitrogen, operating at X-band. The compounds were characterized by ¹H (400.13 MHz) and ¹³C-NMR (100.62 MHz) spectra recorded on a Bruker Avance 400 MHz spectrometer (Bruker BioSpin GmbH, Rheinstetten, Germany) at ≈ 20 °C probe temperature. The internal reference used for the ¹H-NMR measurements in CDCl₃ was tetramethylsilane (TMS) and in D_2O was 3-(trimethylsilyl)propionic acid- d_4 -sodium salt (DSS). Chemical shifts (δ) were given in ppm and coupling constants (J) in Hz. Resonance assignments are based on chemical shift, peak integration and multiplicity for ¹H-NMR spectra and on 2D experiments (COSY, HMQC and HMBC) for ¹³C-NMR spectra. FIDs were processed using the TopSpin software version 3.2 from Bruker.

3.1.1. Reagents

The dimethylester of tiodiglycolic acid (Scheme 1) was prepared according to a reported procedure [22]. Triethylenetetramine, tiodiglycolic acid and borane tetrahydrofuran complex solution 1 M in THF were purchased from Aldrich (Sigma-Aldrich, Madrid, Spain). All the commercially available chemicals were of reagent analytical grade and used as supplied without further purification. Organic solvents were purified or dried by standard methods [52].

3.2. Synthesis of 1-Thia-4,7,10,13-tetraazacyclopentadecane ([15]aneN₄S)

A solution of dimethyl thiodiglycolate (3.03 g, 17 mmol) in dry methanol (100 mL) was added to a solution of triethylenetetramine (2.94 g, 20 mmol) in the same solvent (400 mL), at rt. This mixture was stirred under nitrogen at 40 °C for 9 days. The solvent was then removed under reduced pressure. The remaining oil was dissolved in a minimum amount of chloroform and purified through a silica-gel column (2.5 × 30 cm) using a mixture of CHCl₃–MeOH (20:80 v/v) as eluent. The pure compound was dissolved in methanol and 37% hydrochloric acid was added until pH \approx 3. The cyclic diamide precipitated as an off-yellow salt (2.94 g, 74%). IR (KBr, cm⁻¹): v 3427 (N–H), 1652 (C=O). ¹H-NMR (400.13 MHz; D₂O; DSS; pD = 3.4): δ 3.26 (t, 4H, (triplet), *H_d*) 3.35 (s, 4H, (singlet), *H_a*), 3.53 (t, 4H, *H_c*), 3.57 (s, 4H, *H_e*) ppm. ¹³C-NMR (100.61 MHz; D₂O; dioxane; pD = 3.4): δ 35.3 (*C_c*), δ 37.5 (*C_a*), 42.8 (*C_e*), 48.2 (*C_d*), 175.0 (*C*₂) ppm.

The cyclic diamide (1.10 g, 4,2 mmol) was reduced with a large excess of borane in refluxing dry THF (100 mL) under nitrogen, for eight hours. After reduction, the obtained oil was dissolved in chloroform and purified by silica-gel chromatography. The trihydrocloride salt was obtained by addition of 37% HCl until pH ≈ 2 (0.98 g, 68%). IR (KBr, cm⁻¹): v 3426 (N–H). ¹H-NMR (400.13 MHz; D₂O; DSS; pD = 1.72): δ 3.17 (t, 4H, ³J = 6, H_a), 3.34 (s, 4H, ³J = 6, H_e), 3.44 (t, 4H, H_d), δ 3.50 (t, 4H, ³J = 6, H_b), 3.57 (t, 4H, ³J = 6, H_c) ppm. ¹³C-NMR (100.61 MHz; D₂O; dioxane; pD = 1.72): δ 29.55 (C_a), 43.64 (C_d), 45.00 (C_c), 45.37 (C_e), 46.94 (C_b). m/z (ESI-MS; methanol; positive ion mode) 233.20 [M + H]⁺ (Figures S7–S8 in Supplementary Materials).

3.3. Potentiometric Studies

3.3.1. Reagents and Solutions

All solutions were prepared with demineralized water obtained by a Millipore/Milli-Q system. Solutions of the ligand were prepared at ca. 2.50 × 10⁻³ M and their exact concentrations were obtained by titration with the standardised solution of KOH.

Metal ion solutions were prepared at about 0.050 M from nitrate salts (analytical grade), except in the case of mercury nitrate (*ca*. 0.01 M) that was kept in excess of nitric acid to prevent precipitation. The solutions were standardised by titration with Na_2H_2EDTA [53].

Carbonate-free solutions of the titrant KOH were freshly prepared by dilution of a commercial ampoule of Fixanal (Fluka, Sigma-Aldrich, Madrid, Spain) at *ca*. 0.10 M, under a stream of pure argon gas. Solutions were discarded every time carbonate concentration was about 0.5% of the total amount of base. A 0.100 M standard solution of HNO₃ (prepared from a Merck ampoule) was used for the

back titrations. The titrant solutions were standardised (tested by Gran's method) [54]. For the competition titrations a standard K_2H_2EDTA aqueous solution was used.

The equipment used has been described before [7]. The temperature was controlled at 25.0 ± 0.1 °C. CO₂ was excluded from the titration cell during experiments by passing argon across the experimental solution. The ionic strength of the solutions was kept at 0.10 ± 0.01 M with KNO₃.

3.3.2. Measurements

The $[H^+]$ of the solutions was determined by the measurement of the electromotive force (emf) of the cell, $E = E'' + Q \log[H^+] + E_j$. E'' and Q were determined by titration of a solution of known hydrogen-ion concentration at the same ionic strength, using the acid pH range of the titration. E_j was found to be negligible under our experimental conditions. The value of K_w was obtained from data acquired in the alkaline range of the titration, considering E'' and Q valid for the entire pH range and found to be equal to $10^{-13.80}$ M² in our experimental conditions. The electromotive force data were determined after additions of 0.050 mL increments of standardised KOH solution, and after stabilization in this direction, equilibrium was then approached from the other direction by adding standard 0.100 M nitric acid (back titration). Before and after each determination, a calibration of the system was performed by titration of a 2.00 × 10⁻³ M HNO₃ solution.

The potentiometric equilibrium measurements were carried out using 20.00 mL of $\approx 2.50 \times 10^{-3}$ M ligand solutions diluted to a final volume of 30.00 mL, in the absence of metal ions and in the presence of each metal ion for which the C_M:C_L ratio was 1:1. A minimum of two replicate measurements was made. For the reactions of Cu²⁺ and Hg²⁺, ligand-ligand competition titrations were performed to determine the stability constants. K₂H₂EDTA was used as the second ligand in ratios C_L¹: C_L: C_M 1:0.75:1, being L¹, K₂H₂EDTA [55]. EDTA protonation and copper(II) stability constants values were determined before, under the same experimental conditions: log $K_1^{\rm H} = 10.22$, log $K_2^{\rm H} = 6.16$, log $K_3^{\rm H} = 2.71$, log $K_4^{\rm H} = 2.0$, log $K_{\rm CuEDTA} = 19.23$, log $K_{\rm CuHEDTA} = 3.06$, log $K_{\rm LEDTAOH} = 11.33$ [55]; for the Hg(II) complexes the following values were selected from the literature: log $K_{\rm HgEDTA} = 21.50$, log $K_{\rm HgEDTA} = 3.20$, log $K_{\rm HgEDTAOH} = 8.90$ [56].

3.3.3. Calculation of Equilibrium Constants

Overall equilibrium constants β_i^H and $\beta_{M_mH_hL_l}$ (being $\beta_{M_mH_hL_l} = [M_mH_hL_l]/[M]^m [H]^h [L]^l$) were calculated by fitting the potentiometric data from protonation or complexation titrations with the HYPERQUAD program [34]. Species distribution diagrams were plotted from the calculated constants with the HySS program [37]. Only mononuclear species, ML, MHL and MH_1L were found for the metal complexes of [15]aneN₄S (being $\beta_{MH_1L} = \beta_{MLOH} \times K_w$). The hydrolysis constants of the metal ions were taken from literature and kept constant for the calculations. Differences, in log units, between the values of β_{MHL} (or β_{MH_1L}) and β_{ML} constants, provide the stepwise reaction constants. The species considered in a particular model were those that could be justified by the principles of coordination chemistry. The errors quoted are the standard deviations of the overall stability constants given directly by the program for the input data, which include all the experimental points of all titration curves, and were determined by the normal propagation rules for the stepwise constants.

3.4. Spectroscopic Studies

¹H-NMR titration was performed with a 4.80×10^{-2} M solution of [15]aneN₄S prepared in D₂O. The pD values were adjusted by adding DCl or CO₂-free KOD solutions. Following each addition, the –log [H^{*}] was measured after equilibration, directly in the NMR tube with an Orion 3 Star pH meter equipped with a combined glass Ag-AgCl microelectrode U402-M3-S7/200, Mettler-Toledo (Barcelona, Spain).

The electrode was previously calibrated with standard aqueous buffers solutions and the pD values were calculated according to the equation $pD = pH^* + (0.40 \pm 0.02)$, where pH^* corresponds to the reading of the pH meter [28].

The dissociation constants in D₂O (p*K*_D) were determined from the ¹H-NMR titration by using the HypNMR program [57]. These p*K*_D values were converted to p*K*^H values obtained in water by the equation $pK_D = 0.11 + 1.10 \times pK_H$ [28].

Magnetic moments were measured at 293.6 K using aqueous solutions of Co[15]aneN₄S²⁺ (1.99 × 10⁻³ M, pH 7.02), Ni[15]aneN₄S²⁺ (2.39 × 10⁻³ M, pH 7.11) and Cu[15]aneN₄S²⁺ (3.98 × 10⁻³ M, pH 7.09). The ¹H-NMR spectra of the solutions with DSS as internal reference, were acquired in a tube containing an internal capillary filled with D₂O and DSS, and the corresponding magnetic moments calculated from the shift ($\Delta\delta$) between both reference signals, according to Evans method [38].

Electronic spectra were recorded using aqueous solutions of Co^{2+} , Ni^{2+} and Cu^{2+} complexes for visible-near IR regions of 1.21×10^{-2} M, 1.23×10^{-2} M and 1.29×10^{-2} M at pHs 6.99, 6.98, 7.08, respectively; for UV region 1.02×10^{-3} M, 2.04×10^{-3} M and 2.02×10^{-3} M at pHs 6.92, 6.87 and 7.08, respectively.

EPR spectroscopy measurements of copper(II) complexes of [15]aneN₄S were performed at 104 K. The complexes were prepared in 1.25×10^{-3} M, at pH 4.10, 7.40 and 9.00, in 1 M NaClO₄ aqueous solutions.

4. Conclusions

A thiatetraaza macrocycle [15]aneN₄S having four nitrogen and one sulphur as donor atoms has been synthesised. Potentiometric studies have shown that this compound has a high selectivity towards Hg(II) and Cu(II) over the other divalent metal ions under study. The UV-visible-near IR spectroscopies and magnetic moment data for the Co(II) and Ni(II) complexes indicated a tetragonal distorted coordination geometry for both metal centres. The value of magnetic moment and the X-band EPR spectra of the Cu(II) complex are consistent with a distorted square pyramidal geometry.

This work suggest that [15]aneN₄S should be evaluated as a potential ligand to be used in chelation therapy on disorders triggered by these metal ions. Further studies would be performed in order to evaluate the efficacy of this chelator in the biological milieu.

Supplementary Materials

Supplementary materials can be acceded at: http://www.mdpi.com/1420-3049/19/1/550/s1.

Acknowledgments

The authors acknowledge Rita Delgado and the Instituto de Tecnologia Química e Biológica, Universidade Nova de Lisboa, Portugal, for the UV-visible and EPR spectroscopies. The authors also thank the Fundação para a Ciência e a Tecnologia (FCT) for the project REDE/1518/REM/2005 for ESI-MS/MS experiments at LCLEM, Faculdade de Farmácia, Universidade de Lisboa, Portugal.

Conflicts of Interest

The authors declare no conflict of interest.

References

- 1. Hayes, R.B. The carcinogenicity of metals in humans. Cancer Cause. Control 1997, 8, 371-385.
- 2. Järup, L. Hazards of heavy metal contamination. Br. Med. Bull. 2003, 68, 167–182.
- 3. Caussy, D.; Gochfeld, M.; Gurzau, E.; Neagu, C.; Ruedel, H. Lessons from case studies of metals: Investigating exposure, Bioavailability, and risk. *Ecotoxicol. Environ. Saf.* **2003**, *56*, 45–51.
- 4. Blanuša, M.; Varnai, V.M.; Piasek, M.; Kostial, K. Chelators as antidotes of metal toxicity: Therapeutic and experimental aspects. *Curr. Med. Chem.* **2005**, *12*, 2771–2794.
- 5. Flora, S.J.S.; Pachauri, V. Chelation in metal intoxication. *Int. J. Environ. Res. Public Health* 2010, 7, 2745–2788.
- 6. Sears, M.E. Chelation: Harnessing and enhancing heavy metal detoxification—A review. *Sci. World J.* **2013**, *2013*, 1–13.
- Fernandes, A.S.; Cabral, M.F.; Costa, J.; Castro, M.; Delgado, R.; Drew, M.G.; Felix, V. Two macrocyclic pentaaza compounds containing pyridine evaluated as novel chelating agents in copper(II) and nickel(II) overload. *J. Inorg. Biochem.* 2011, *105*, 410–419.
- 8. Andersen, O.; Aaseth, J. Molecular mechanisms of *in vivo* metal chelation: Implications for clinical treatment of metal intoxications. *Environ. Health. Perspect.* **2002**, *110*, 887–890.
- 9. Andersen, O. Chemical and biological considerations in the treatment of metal intoxications by chelating agents. *Mini Rev. Med. Chem.* **2004**, *4*, 11–21.
- Aposhian, H.V.; Maiorino, R.M.; Gonzalez-Ramirez, D.; Zuniga-Charles, M.; Xu, Z.; Hurlbut, K.M.; Junco-Munoz, P.; Dart, R.C.; Aposhian, M.M. Mobilization of heavy metals by newer, Therapeutically useful chelating agents. *Toxicology* 1995, 97, 23–38.
- Gonçalves, S.; Fernandes, A.S.; Oliveira, N.G.; Marques, J.; Costa, J.; Cabral, M.F.; Miranda, J.; Cipriano, M.; Guerreiro, P.S.; Castro, M. Cytotoxic effects of cadmium in mammary epithelial cells: Protective role of the macrocycle [15]pyN5. *Food Chem. Toxicol.* 2012, *50*, 2180–2187.
- 12. Mewis, R.E; Archibald, S.J. Biomedical applications of macrocyclic ligand complexes. *Coord. Chem. Rev.* **2010**, *254*, 1686–1712.
- 13. Hancock, R.D.; Martell, A.E. Ligand design for selective complexation of metal ions in aqueous solution. *Chem. Rev.* **1989**, *89*, 1875–1914.
- 14. Hancock, R.D.; Dobson, S.M.; Boeyens, J.C.A. Metal ion size selectivity of 1-Thia-4, 7-diazacyclononane (9-aneN₂S), and other tridentate macrocycles. A study by molecular

mechanics calculation, structure determination, and formation constant determination of complexes of 9-aneN₂S. *Inorganica Chim. Acta* **1987**, *133*, 221–231.

- Westerby, B.C.; Juntunen, K.L.; Leggett, G.H.; Pett, V.B.; Koenigbauer, M.J.; Purgett, M.D.; Taschner, M.J.; Ochrymowycz, L.A.; Rorabacher, D.B. Macrocyclic polyamino polythiaether ligands with N_xS_{4-x} and N_xS_{5-x} donor sets: Protonation constants, stability constants, and kinetics of complex formation with the aquocopper(II) ion. *Inorg. Chem.* **1991**, *30*, 2109–2120.
- Arnaud-Neu, F.; Schwing-Weill, M.J.; Louis, R.; Weiss, R. Thermodynamic and spectroscopic properties in aqueous solutions of pentadentate macrocyclic complexes. *Inorg. Chem.* 1979, 18, 2956–2961.
- Balakrishnan, K.P.; Kaden, T.A.; Siegfried, L.; Zuberbühler, A.D. Stabilities and redox properties of Cu(I) and Cu(II) complexes with macrocyclic ligands containing the N₂S₂ donor set. *Helv. Chim. Acta* 1984, 67, 1060–1069.
- Walker, T.L.; Malasi, W.; Bhide, S.; Parker, T.; Zhang, D.; Freedman, A.; Modarelli, J.M.; Engle, J.T.; Ziegler, C.J.; Custer, P.; *et al.* Synthesis and characterization of 1,8-dithia-4,11diazacyclotetradecane. *Tetrahedron Lett.* 2012, *53*, 6548–6551.
- Papini, G.; Alidori, S.; Lewis, J.S.; Reichert, D.E.; Pellei, M.; Lobbia G.G.; Biddlecombe, G.B.; Anderson, C.J.; Santini, C. Synthesis and characterization of the copper(II) complexes of new N₂S₂-donor macrocyclic ligands: Synthesis and *in vivo* evaluation of the ⁶⁴Cu complexes. *Dalton Trans.* 2009, 7, 177–184.
- Aquilanti, G.; Giorgetti, M.; Minicucci, M.; Papini, G.; Pellei, M.; Tegoni, M.; Trasatti, A.; Santini, C. A study on the coordinative versatility of new N,S-donor macrocyclic ligands: XAFS, and Cu²⁺ complexation thermodynamics in solution. *Dalton Trans.* 2011, 40, 2764–2777.
- Kodama, M.; Koike, T.; Hoshiga, N.; Machida, R.; Kimura, E. Metal chelates of sulphur-containing polyamine macrocycles and oxygenation of the corresponding cobalt(II) complexes. *J. Chem. Soc. Dalton Trans.* 1984, 673–678.
- 22. Vollhardt, K.P.C.; Schore, N.E. Organic Chemistry, 6th ed.; Freeman and Co.: New York, NY, USA, 2011.
- 23. Tabushi, I.; Okino, H.; Kuroda, Y. Convenient synthesis of macrocyclic-compounds containing two of nitrogen, Oxygen or sulphur atoms. *Tetrahedron Lett.* **1976**, *17*, 4339–4342.
- Steenland, M.W.A.; Westbroek, P.; Dierck, I.; Herman, G.G.; Lippens, W.; Temmerman, E.; Goeminne, A.M. Aqueous solution study of Cu(II) and Ni(II) complexes of macrocyclic oxa- and thia- containing trans-dioxo-tetraamines. *Polyhedron* 1999, *18*, 3417–3424.
- 25. Bencini, A.; Bianchi, A.; Garcia-España, E.; Micheloni, M.; Ramirez, J.A. Proton coordination by polyamine compounds in aqueous solution. *Coord. Chem. Rev.* **1999**, *188*, 97–156.
- 26. Cabral, M.F.; Delgado, R. Metal complexes of pentadentate macrocyclic ligands containing oxygen and nitrogen as donor atoms. *Helv. Chim. Acta* **1994**, 77, 515–524.
- 27. Motekaitis, R.J.; Rogers, B.E.; Reichert, D.E.; Martell, A.E.; Welch, M.J. Stability and structure of activated macrocycles. Ligands with biological applications. *Inorg. Chem.* **1996**, *35*, 3821–3827.
- Delgado, R.; Fraústo da Silva, J.J.R.; Amorim, M.T.S.; Cabral, M.F.; Chaves, S.; Costa, J. Dissociation constants of Brønsted acids in D₂O and H₂O: Studies on polyaza and polyoxa-polyaza macrocycles and a general correlation. *Anal. Chim. Acta* 1991, 245, 271–282.

- Hancock, R.D.; Wade, P.W.; Ngwenya, M.P.; de Sousa, A.S.; Damu, K.V. Ligand design for complexation in aqueous solution. 2. Chelate ring size as a basis for control of size-based selectivity for metal ions. *Inorg. Chem.* 1990, 29, 1968–1974.
- Riley, D.P.; Henke, S.L.; Lennon, P.J.; Weiss, R.H.; Neumann, W.L.; Rivers, W.J., Jr.; Aston, K.W.; Sample, K.R.; Rahman, H.; Ling, C.S.; *et al.* Synthesis, characterization, and stability of manganese(II) C-substituted 1,4,7,10,13-pentaazacyclopentadecane complexes exhibiting superoxide dismutase activity. *Inorg. Chem.* 1996, 35, 5213–5231.
- Kodama, M.; Kimura, E. Effects of axial ligation on molecular oxygen binding by donor atoms built in saturated macrocycles. Equilibrium and kinetic study with cobalt(II) complexes of macrocyclic pentaamines and oxatetraamine. *Inorg. Chem.* 1980, 19, 1871–1875.
- 32. Kodama, M.; Kimura, E.; Yamaguchi, S. Complexation of the macrocyclic hexa-amine ligand 1,4,7,10,13,16-hexa-azacyclo-octadecane("18-azacrown-6"). *J. Chem. Soc. Dalton Trans.* **1980**, 2536–2538.
- 33. Kodama, M.; Kimura, E. Equilibria of complex formation between several bivalent metal ions and macrocyclic tri- and penta-amines. *J. Chem. Soc. Dalton Trans.* **1978**, 1081–1085.
- 34. Gans, P.; Sabatini, A.; Vacca, A. Investigation of equilibria in solution. Determination of equilibrium constants with the HYPERQUAD suite of programs. *Talanta* **1996**, *43*, 1739–1753.
- 35. Kodama, M.; Kimura, E. Effects of cyclization and ring size on complex formation between penta-amine ligands and copper(II). *J. Chem. Soc. Dalton Trans.* **1978**, 104–110.
- 36. Costa, J.; Delgado, R.; Drew, M.G.B.; Félix, V. Design of selective macrocyclic ligands for the divalent first-row transition-metal ions. *J. Chem. Soc. Dalton Trans.* **1998**, 1063–1071.
- Alderighi, L.; Gans, P.; Ienco, A.; Peters, D.; Sabatini, A.; Vacca, A. Hyperquad simulation and speciation (HySS): A utility program for the investigation of equilibria involving soluble and partially soluble species. *Coord. Chem. Rev.* 1999, *184*, 311–318.
- 38. Evans, D.F. The determination of the paramagnetic susceptibility of substances in solution by nuclear magnetic resonance. *J. Chem. Soc.* **1959**, 2003–2005.
- 39. Lever, A.B.P. *Inorganic Electronic Spectroscopy*, 2nd ed.; Elsevier: Amsterdam, The Netherlands, 1984.
- 40. Banci, L.; Bencini, A.; Benelli, C.; Gatteschi, D.; Zanchini, C. Spectral-structural correlations in high-spin cobalt(II) complexes. *Sruct. Bond.* **1982**, *52*, 37–86.
- 41. Bertini, I.; Luchinat, C. High spin cobalt(II) as a probe for the investigation of metalloproteins. *Adv. Inorg. Biochem.* **1984**, *6*, 71–111.
- 42. Martin, L.Y.; Sperati, C.R.; Busch, D.H. The spectrochemical properties of tetragonal complexes of high spin nickel(II) containing macrocyclic ligands. *J. Am. Chem. Soc.* **1977**, *99*, 2968–2981.
- Sacconi, L.; Mani, F.; Bencini, A. Nickel. In *Comprehensive Coordination Chemistry*; Wilkinson, G., Gillard, R.D., McCleverty, J.A., Eds.; Pergamon Press: Oxford, UK, 1987; pp. 1–137.
- 44. Neese, F. Electronic Structure and Spectroscopy of Novel Copper Chromophores in Biology. Diploma Thesis, University of Konstanz, Konstanz, Germany, June 1993.
- Fernandes, A.S.; Gaspar, J.; Cabral, M.F.; Caneiras, C.; Guedes, R.; Rueff, J.; Castro, M.; Costa, J.; Oliveira, N.G. Macrocyclic copper(II) complexes: Superoxide scavenging activity, Structural studies and cytotoxicity evaluation. *J. Inorg. Biochem.* 2007, *101*, 849–858.

- Li, Y. X-Ray structures and spectroscopic studies of diaqua- and dichlorocopper(II) complexes of 15 crown 5 and 4' substituted benzo-15-Crown-5 with a 3dx(x=z2) ground state doublet. *Bull. Chem. Soc. Jpn.* 1996, 69, 2513–2523.
- Barbaro, P.; Bianchini, C.; Capannesi, G.; di Luca, L.; Laschi, F.; Petroni, D.; Salvadori, P.A.; Vacca, A.; Vizza, F. Synthesis and characterization of the tetraazamacrocycle 4,10-dimethyl-1,4,7,10-tetraazacyclododecane-1,7-diacetic acid (H₂Me₂DO2A) and of its neutral copper(II) complex [Cu(Me₂DO2A)]. A new ⁶⁴Cu-labeled macrocyclic complex for positron emission tomography imaging. *J. Chem. Soc. Dalton Trans.* **2000**, 2393–2401.
- 48. Hathaway, B.J. Copper. Coord. Chem. Rev. 1983, 52, 87-169.
- 49. Gersmann, H.R.; Swalen, J.D. Electron paramagnetic resonance spectra of copper complexes. *J. Chem. Phys.* **1962**, *36*, 3221–3233.
- 50. Yokoi, H.; Sai, M.; Isobe, T.; Ohsawa, S. ESR studies of the copper(II) complexes of amino acids. *Bull. Chem. Soc. Jpn.* **1972**, *45*, 2189–2195.
- 51. Lau, P.W.; Lin, W.C. Electron spin resonance and electronic structure of some metalloporphyrins. *J. Inorg. Nucl. Chem.* **1975**, *37*, 2389–2398.
- 52. Perrin, D.D.; Armarego, W.L.F. *Purification of Laboratory Chemicals*, 3rd ed.; Pergamon Press: Oxford, UK, 1988.
- 53. Schwarzenbach, G.; Flaschka, W. *Complexometric Titrations*, 2nd ed.; Methuen & Co: London, UK, 1969.
- 54. Rossotti, F.J.C.; Rossotti, H. Potentiometric titrations using Gran plots: A textbook omission. *J. Chem. Educ.* **1965**, *42*, 375–378.
- 55. Delgado, R.; do Carmo Figueira, M.; Quintino, S. Redox method for the determination of stability constants of some trivalent metal complexes. *Talanta* **1997**, *45*, 451–462.
- 56. Pettit, L.D.; Powell, H.K.J. *IUPAC Stability Constants Database*; Academic Software: Timble, Otley, Yorks, UK, 2003.
- Frassineti, C.; Ghelli, S.; Gans, P.; Sabatini, A.; Moruzzi, M.S.; Vacca, A. Nuclear magnetic resonance as a tool for determining protonation constants of natural polyprotic bases in solution. *Anal. Biochem.* 1995, 231, 374–382.

Sample Availability: Not available.

© 2014 by the authors; licensee MDPI, Basel, Switzerland. This article is an open access article distributed under the terms and conditions of the Creative Commons Attribution license (http://creativecommons.org/licenses/by/3.0/).